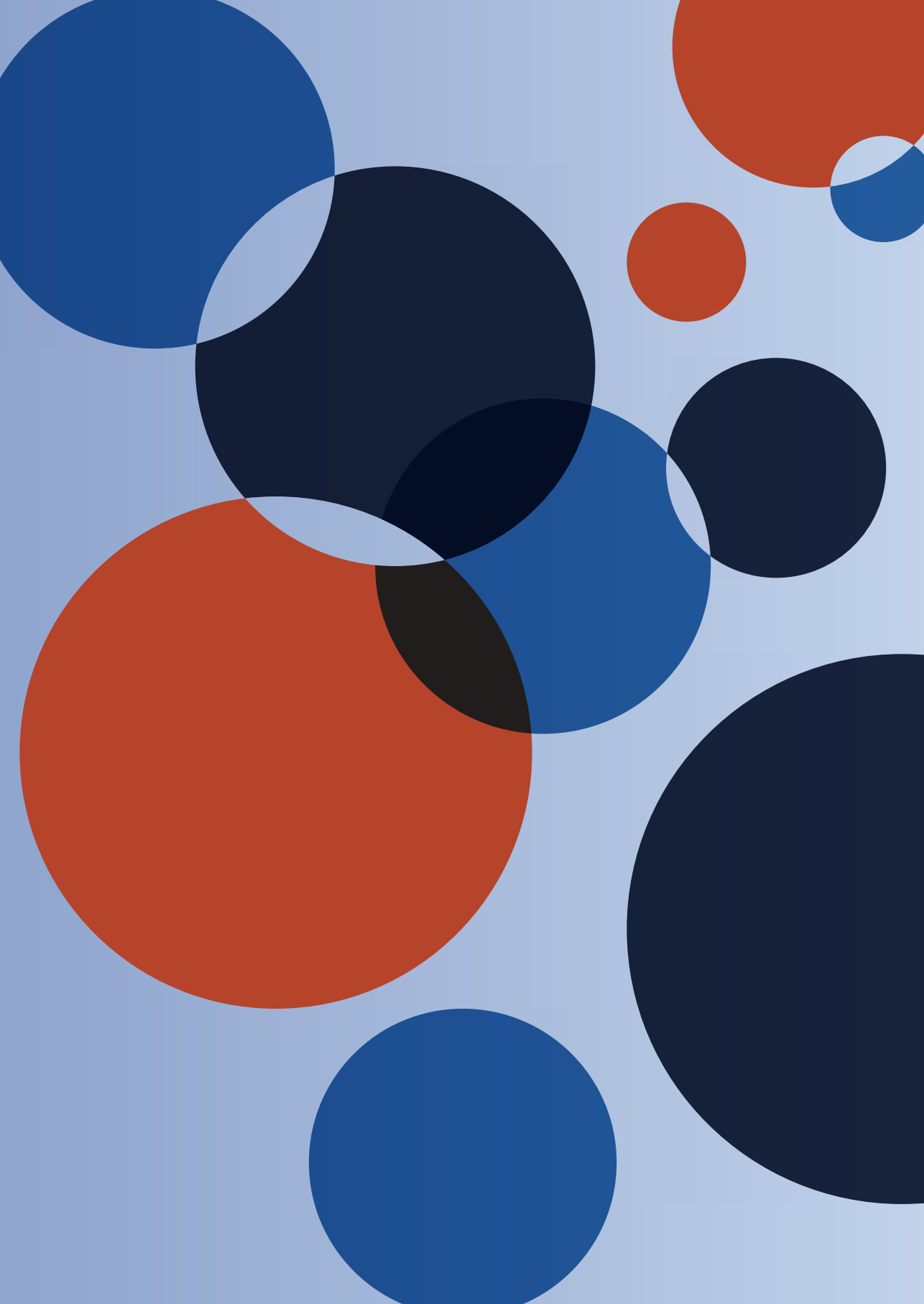

PLASMA PROTEIN SIGNATURES OF A MURINE VENOUS THROMBOSIS MODEL AND SLC44A2 KNOCKOUT MICE USING QUANTITATIVE-TARGETED PROTEOMICS

Julia Tilburg, Sarah A. Michaud, Chrissta X. Maracle, Henri H. Versteeg, Christoph H. Borchers, Bart J.M. van Vlijmen*, Yassene Mohammed*
*: These authors contributed equally

Thromb Haemost. 2020 Mar;120(3):423-436.

4

Abstract

The plasma compartment of the blood holds important information on the risk to develop cardiovascular diseases such as venous thrombosis (VT). Mass spectrometry-based targeted proteomics with internal standards quantifies proteins in multiplex allowing generation of signatures associated with a disease or a condition. Here, to demonstrate the method, we investigate the plasma protein signatures in mice following the onset of VT which was induced by RNA interference targeting the natural anticoagulants antithrombin and protein C. We then study mice lacking SLC44A2 which was recently characterized as a VT-susceptibility gene in human genome-wide association studies. We use a recently developed panel of 375 multiplexed mouse protein assays measured by mass spectrometry. A strong plasma protein signature was observed when VT was induced. Discriminators included acute phase response proteins, and proteins related to erythrocyte function. In mice lacking SLC44A2, protein signature was primarily overruled by the difference between sexes and not by the absent gene. Upon separate analyses for males and females, we were able to establish a signature for *Slc44a2* deficiency, in which glycosylation-dependent cell adhesion molecule-1 and thrombospondin-1 were shared by both sexes. The minimal impact of *Slc44a2* deficiency on the measured plasma proteins suggests that the main effect of SLC44A2 on VT does not lay ultimately in the plasma compartment. This suggests further investigation into the role of this VT-susceptibility gene should perhaps also question the possible involvement in cellular mechanisms.

Introduction

Venous thrombosis (VT), i.e. unwanted clotting of the blood within a vein, is a complex cardiovascular disease and its pathogenesis is not completely understood (1, 2). The plasma compartment of the blood, which provides the clotting factors involved in VT, holds important information on the risk to develop VT (3). Several clotting factors i.e. pro- and anticoagulant proteins, as well as pro- and antifibrinolytic proteins are affected by genetic and acquired risk for VT (4, 5). Plasma levels and activity of these proteins are important in assessing VT risk, and contribute to understanding how genetic and acquired risk factors relate to VT (3, 4). In addition, there is increasing evidence supporting that also proteins not belonging to coagulation and fibrinolytic pathways may play a role in VT, including proteins involved in inflammation, the complement system, or lipoprotein metabolism (6-10).

Recently, a meta-analysis of genome-wide association studies (GWASs) revealed two novel genetic susceptibility loci for VT (5). Interestingly, these loci harbor genes encoding proteins that cannot directly be linked to coagulation. Among these was a VT locus encompassing the *SLC44A2* gene, located on 19p13.2, which was associated with thrombotic events also in a second independent GWAS cohort (11). SLC44A2 encodes the solute carrier family 44 member 2 protein (SLC44A2), a poorly characterized gene, and regarding a mechanism underlying the association between SLC44A2 and VT can, at present, only be speculated. So far no links to coagulation- and fibrinolysis-related pathways could be identified (5) apart from an interaction of SLC44A2 with von Willebrand factor (VWF) as identified in *in vitro* studies (12).

To understand the role of SLC44A2 in VT we previously undertook an animal approach using recently generated *Slc44a2* deficient (*Slc44a2-/-)* mice (13). Compared with their wild type (*Slc44a2+/+)* littermates these *Slc44a2-/-* mice revealed no differences in the measured coagulation related parameters, i.e. thrombin generation, transcriptional profiling of coagulation related genes, multimerization and localization within venous and arterial vessels, with the exception of a modest decrease in plasma VWF level (14). These first observations encourage to further explore the link between SLC44A2 and VT in and outside of coagulation- and fibrinolysis-related pathways using more in depth analysis.

As an alternative to individual activity- or antibody-based plasma protein assays, mass spectrometry(MS)-based proteomics allows deeper investigation of the proteome in relation to health and disease (15-20). The levels of several coagulation proteins can be measured in plasma and serum by MS (21, 22) as well as secreted proteins that are unrelated to the coagulation cascade but associated with VT risk (23). Detection of venous thromboembolism signature in serum using proteomics was previously demonstrated (24) as well as in depth analysis of VT proteomics using *ex vivo* prepared fibrin clots (25). In mouse, various studies demonstrated phenotyping of disease models using proteomics, showing also evidence of an age and sex dependent plasma proteome (26, 27). We recently demonstrated that

MS-based targeted proteomics with stable-isotope-labeled internal standards can be used for rapid, multiplexed, and precise quantification of coagulation- and fibrinolysis-related plasma proteins in human using as small volumes as less than 10 µL of plasma (28, 29). We were able to capture plasma protein signature information on VT, in particular VT and cancer, which was not obvious from single measurements by the conventional assays. Contrary to traditional protein phenotyping techniques, MS-based targeted proteomics can be highly multiplexed without sacrificing specificity nor quantitative precision (30). This allows measuring abundance of hundreds of proteins in hundreds of samples in standardized way facilitating best comparative analysis.

Recently, hundreds of MS-based targeted proteomics assays for various mouse proteins have been developed and validated (26). This opens up the opportunity to measure abundances of many mouse proteins for which traditional techniques like antibody assays are currently not available, nor feasible. In addition, it allows capturing plasma protein signature information associated with genes or disease in an experimental mouse setting using low volumes of samples, which is a limitation in small animals like mice. In the present study, we use these assays to extend our analysis beyond traditional coagulation factors and measure additional plasma proteins.

First, we measured plasma protein levels in mice where VT follows RNA interference-mediated imbalance in natural anticoagulation (31, 32). Although one can question its suitability as best VT model mimicking human disease, we chose to use this model as it presents a strong venous thrombotic phenotype, coincides with clinical signs and changes in clotting tests. As a result, changes in abundance of various plasma proteins are expected. Next, we determined protein levels in plasma samples from seemingly normal *Slc44a2* deficient mice to investigate any possible protein signature for this less-characterized VT-susceptibility gene. Putting the results of both experiments side by side, i.e. changes in plasma protein levels in induced VT and *Slc44a2* knockout mice, can give an indication to the level to which the *Slc44a2* absence affect plasma proteins. A strong signature in plasma protein abundances was observed when VT was induced including acute phase response and erythrocyte-specific proteins. In mice lacking *Slc44a2,* the plasma protein signature was overruled by the sex of the mice and not by the absent gene. When stratifying for sex, we were able to establish a signature for *Slc44a2* deficiency represented in glycosylation-dependent cell adhesion molecule-1 and thrombospondin-1. Both these proteins are associated with cell-cell interactions, which suggests that the role of *Slc44a2* lays outside of the plasma and perhaps question possible involvement of this VT-susceptibility gene in cellular mechanisms.

Materials and Methods

Mice

Female C57BL/6J mice aged 6 weeks were obtained from Charles River, Maastricht, The Netherlands. Mice deficient for solute carrier family 44 member 2 protein (*Slc44a2-/-*, gene

located on mouse chromosome 9) were previously generated by crossing mice with *Slc44a2* exon 3 to 10 flanked by LoxP sites with deleter EIIa-Cre transgenic mice (13, 14). Mice were genotyped for presence of the *Slc44a2* knockout allele using ear biopsy DNA as previously described (14). Offspring, heterozygous for the *Slc44a2* knockout allele (*Slc44a2*+/-), was used for backcrossing to C57BL/6J (at least seven generations). Subsequently, interbreeding of the *Slc44a2*+/- mice yielded male and female *Slc44a2*-/- and wild type littermate control *Slc44a2*+/+ mice which were used for blood and tissue collection (at 15 weeks of age, N=8 for female *Slc44a2*+/+ and weight at euthanasia 21.75 ± 2.14 g, N=8 for female *Slc44a2*-/- mice and weight at euthanasia 22.36 ± 1.14 g, N=8 for male *Slc44a2*+/+ and weight at sacrifice 29.82 ± 5.51 g, and N=7 for male *Slc44a2*-/- mice and weight at euthanasia 29.22 ± 1.70 g). All mice in this study were housed under standard conditions with free access to water and food. All experiments were approved by The Netherlands National Animal Welfare Committee, under project license number AVD106002016607.

Induction of venous thrombosis

Small interfering RNAs (siRNAs) targeting mouse antithrombin (siAT, cat. #S62673, Ambion, Life Technologies, CA, USA) and protein C (siPC(31), cat. #S72192) and a negative control siRNA referred to as siControl (cat. #4404020) were complexed with Invivofectamine® 3.0 (Invitrogen, Life Technologies, CA, USA) exactly according to the procedure provided by the manufacture. A mixture of complexed siAT and siPC (siAT/PC) was prepared in PBS with a final concentration of 4.2 nmol per mL for both siAT and siPC (total 8.4 nmol/mL). The complexed siControl was diluted in PBS to a final concentration of 8.4 nmol/mL. The siAT/PC and siControl were injected intravenously (tail vein) of the 6-week-old female C57BL/6J mice (200 µL per mouse i.e., a total of 1.7 nmol siRNA per mouse, N=8 for siAT/PC and weight at injection was 20.77 ± 1.11 g, and N=7 for siControl and weight at injection was 20.19 ± 0.82 g). The spontaneous venous thrombotic phenotype that follows injection of siAT/PC has been described previously (31, 32). As soon as a siAT/PC injected mouse presented the typical externally visible clinical signs that coincide with the VT phenotype, it was euthanized together with one mouse randomly selected from the siControl injected control group.

Blood collection and processing

For euthanasia, animals were anesthetized using a mixture of ketamine (40 mg/mL, A.A.-Vet, Biddinghuizen, The Netherlands), xylazine (5 mg/mL, Dechra, Northwich, United Kingdom), and atropine (0.1 mg/mL, Pharmachemie BV, Haarlem, The Netherlands) in PBS (indicated are end concentrations) injected subcutaneously at a volume of 75 and 125 µL for females and males, respectively. Before euthanasia, 20 µL of water was added to dipotassium ethylenediaminetetraacetic acid (K_2EDTA) coated vials (average of 1mg K_2EDTA/vial, ref: 365975, BD, NJ, USA), vortexed to dissolve the K_2EDTA, and transferred quantitatively into 1-mL syringes with 24-gauge needle. The anesthetized animal's abdomen was opened, the inferior vena cava exposed and 350 (from animals injected with siControl or siAT/PC) or 500 µL of blood (from *Slc44a2*-/- and *Slc44a2*+/+ males and females) was collected using the K_2EDTA-loaded 1-mL syringe within approximately 15 to 30 seconds. Blood was thoroughly

but carefully mixed with the K_2EDTA within the syringe, and transferred to the original K_2EDTA vials (allowing mixture with possible residual K_2EDTA, and kept on ice until centrifugation). Vena cava and abdominal aorta were cut, allowing euthanasia. Ice-cold blood samples were visually inspected for signs of clotting (absent for all samples) and centrifuged for 5 minutes at 10,000 rpm at 4°C in an Eppendorf Centrifuge 5417R. From the plasma fraction, aliquots were snap frozen in liquid nitrogen, stored at -80°C, shipped on dry ice to the University of Victoria, Canada, and stored again at -80°C until use. *Slc44a2* status was confirmed with PCR on tail tip DNA and at transcript level from the liver transcriptome by quantitative PCR using β-actin (*Actb*) as a reference as described previously (14, 33).

Targeted proteomics

We used 375 validated protein assays in a setting of experimental VT and altered VT-susceptibility. These proteins are measured in a multiplexed experiment and are related to various pathways and, besides their biological relevance reported in literature, they were selected after careful validation for detectability and quantifiably in mouse blood plasma (Table S1, Figure S1)(26). Indeed, proteomics as a field offers other approaches like semi-quantitative bottom-up proteomics that allows detection of more proteins (34). We opted for a targeted proteomics with internal standard approach to achieve best specificity and highest precision, using validated assays for predefined limited–yet expandable–number of proteins. This choice is mainly to achieve best possible comparability between samples.

A total of 375 proteins and their surrogate peptides are listed in supplementary Table S1. The assays are highly multiplexed and standardized consisting of 3 panels of 125 assays each running in parallel in multiple reaction monitoring (MRM) mode and cover various pathways and molecular functions (Figure S1 and Table S1). The development and validation of these assays were performed previously as part of the Proteomics Centre at the University of Victoria efforts to build a library of targeted proteomics assays for profiling mouse plasma and tissues (26, 35, 36). The peptides for the MRM assays were selected using PeptidePicker and synthesized at the University of Victoria Proteomics Centre (37). The sample preparation was performed using a Tecan Freedom Evo 150 robot. The urea-based preparation protocol used was developed and applied previously (38).

The samples were separated on-line with an ultra-high performance liquid chromatography column (EclipsePlusC18 RRHD 150 x 2.1 mm i.d., 1.8 µm particle diameter; Agilent) maintained at 50°C. Peptide separation was performed at 0.4 mL/minute over a 56 minute run, using a multi-step LC gradient (1.5-81% to 2-80% mobile phase B; mobile phase B: 0.1% formic acid in acetonitrile). The exact gradient was as follows (time point in min, solution B %): 0 minutes, 2%; 2 minutes, 7%; 50 minutes, 30%; 53 minutes, 45%, 53.5 minutes, 80%; 55.5 minutes, 80%; 56 minutes, 2%. The LC system was interfaced to a triple-quadrupole mass spectrometer Agilent 6495 via a standard-flow electrospray ionization source and operated in the positive ion mode.

Data processing and analysis

We inspected all response peaks using Skyline software (39) to ensure correct retention time, accurate selection and integration, and uniformity of peak shape for the endogenous and internal standard peptide signals. We calculated the relative peak area ratio of the endogenous to the heavy labeled internal standard peptide. Using this ratio and the known concentration of internal standard peptides, we determined the concentration of the endogenous peptides in the sample by comparison to a standard curve generated in pooled sample (29), for which we used 1/x2 regression weighting. For all hierarchical agglomerative clustering, we used Ward's algorithm (40, 41) on the Euclidean's distances of the scaled and centered determined protein concentrations. All data analysis and visualization were performed using own routines written in R statistical language. For the selection of best discriminating proteins, we used Wilcoxon's signed-rank test.

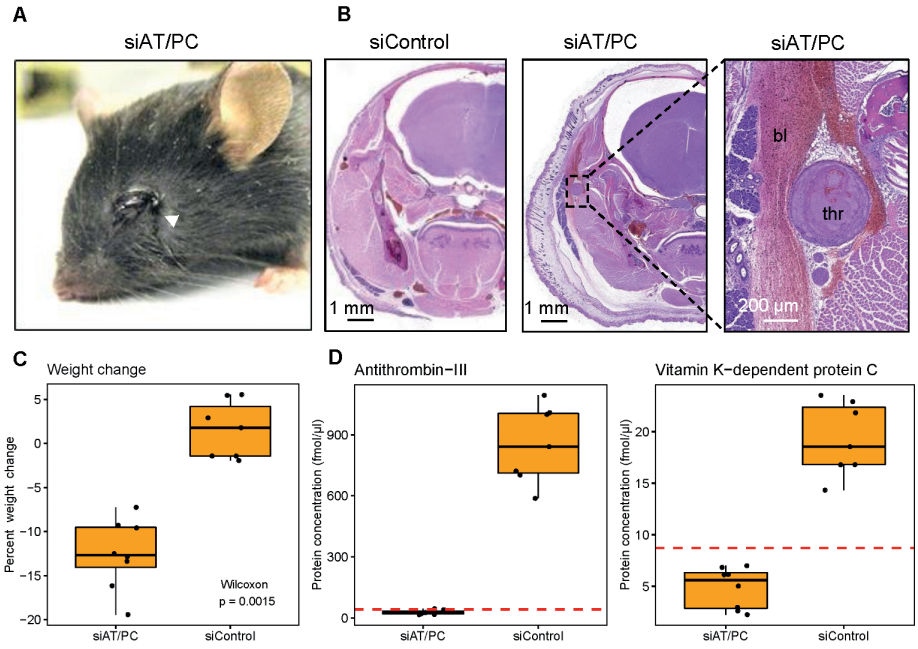

Figure 1. Venous thrombosis in mice 48 to 72 hours after intravenous injection of siRNA targeting antithrombin and protein C (siAT/PC) or control siRNA (siControl). N=8 for siAT/PC and N=7 for siControl. **(A)** Eye of an siAT/PC-treated animal. Unilateral exophthalmos and periocular hemorrhages are shown (arrow head). **(B)** Hematoxylin and eosin staining of coronal head section (5 µm) of mice treated with siAT/PC and siControl, thrombus (thr) and bleeding (bl) are indicated. **(C)** Weight change at euthanasia of mice treated with siAT/PC and siControl relative to weight at siRNA injection (complete information on the weight of all mice are in Table S2 and Table S3). Statistics using Wilcoxon's rank sum test. **(D)** Plasma protein concentration of antithrombin (left) as well as protein C (right) in siAT/PC and siControl mice. PC, protein C; siRNA, small interfering RNA; AT, antithrombin.

Results

Induced venous thrombosis and Slc44a2 deficiency in mice

We applied quantitative targeted proteomics to determine abundance of 375 proteins in plasma samples collected from mice that developed VT following injection of siRNAs targeting antithrombin and protein C (siAT/PC) or control siRNA (siControl). In line with previous observations (31, 32), within 3 days post injection all siAT/PC treated mice developed the typical externally visible clinical signs of VT i.e. unilateral lesions around the eye, edema, and swellings in the head (Figure 1A). Histologically, this presents as a thrombotic coagulopathy (Figure 1B). Additionally, the siAT/PC-treated mice showed expected loss in body weight as compared with their control (P-value=0.0015, Figure 1C). Despite this phenotype, the mice remained lively and did not become lethargic, unresponsive to stimuli, or hypothermic, which may occur upon phenotype progression (31). Effectiveness of antithrombin and protein C silencing was confirmed at the plasma protein level (Figure 1D, described in more detail below). In a parallel experiment, to investigate the effect of the novel thrombosis-susceptibility gene *Slc44a2*, we used *Slc44a2* deficient (-/-) mice and their wild type (+/+) littermates as controls (these mice were all healthy and were not subjected to siAT/PC-induced VT). Upon euthanasia, after *Slc44a2* liver transcript analysis (data not shown), and subsequent re-genotyping at the level of tail tip DNA (data not shown), one knockout male appeared to be heterozygous (*Slc44a2+/-)*. This mouse was included in the plasma proteomics sample measurement, but was later excluded during the data analysis.

Quantification of mouse plasma proteins

In 49 plasma samples (46 mice with 3 measured in duplicate as quality control), we determined the abundance of 375 proteins, which equals a total of 18,375 measurements that were performed on our LC-MS system within a week. The three duplicates were included at origin to control for all aspects of sample handling, shipment, wet laboratory preparation, and measurement. In addition, seven in-house quality controls (pooled mouse plasmas from C57BL/6 mice of both sexes) were included. All measurements were performed in a blinded fashion and the samples were randomized on a 96-well plate to rule out possible batch effects. From the 375 protein assays that were validated and successfully measured in previous mouse experiments (26), 221 proteins passed our stringent quantifiability criteria in the current study, while 154 proteins were below the lower limit of quantification in at least 37 of the 47 samples measured, that is, 80%. This is not necessary a reason to consider these measurements failed. They could still be indicative and the reason to be on the lower side in protein concentration can be related to the experimental intervention, experimental setting, and/or genetics. In addition, our panel includes proteins which are not necessary found in plasma under healthy conditions. For example, the majority of the proteins are not detectable in both male and female control mice cover various molecular functions that are not native to plasma (Figure S1 and Table S1).

Although it was not our main objective to compare the two experimental groups (induced VT and *Slc44a2* deficiency) when looking at all measured samples together using hierarchical clustering (Figure S2), we observed that the strongest discrimination corresponds to the "experimental group". Each experimental group forms its own cluster, the siRNA-treated mice (orange in the first annotation bar, bottom), the *Slc44a2* deficient mice and their controls (green, middle), and the in-house quality controls (blue, top). One single outlier from the female siControl group showed more similarity to wild type *Slc44a2* group from the same sex. Within the siRNA-treated group, a clear distinction was observed between mice treated with siAT/PC, which developed VT and the siControl treated mice, which remained fully healthy, as can be seen in the second annotation bar. In the *Slc44a2* group, we observed a clear distinction between males and females as can be seen in the sex annotation bar, while a clustering based on *Slc44a2*–forth annotation bar–is not observable. The one male *Slc44a2+/-* clusters with the rest of the male mice, but was later removed from the data analysis and interpretation. Including all samples in this comparison allowed a fast check on the data collected and showed that unsupervised clustering on all measured proteins is able to capture clusters based on the presence of VT as well as sex, but not on *Slc44a2* status. In other words, the *Slc44a2* absence does not influence the plasma proteins as strongly as induced VT or sex.

Protein profile (dis)similarities

In order to assess the protein profile similarities in and between groups and samples, we opted to comparing the Pearson's correlation coefficients pairwise between each two samples. When referring to protein profiles, we consider here the proteins that were quantitatively measured in our experiment, although the detectable plasma proteome is indeed larger with over a thousand proteins (42). There were few general observations that stood out. With regard to the three duplicates which were included at origin, a very high correlation of >99% was determined between duplicates (Figure 2A). This confirms the robustness of our method in capturing the similarity in the quantifiable protein profiles. The histogram in Figure 2B shows two distinct distributions of the correlation factors separated around 95%. *Slc44a2-/-* and *Slc44a2+/+* samples were very similar and show a correlation centered around 97%, while those from siAT/PC versus siControl as well as *Slc44a2* knockout were with lower correlation values centered around 92%. This implies that samples from animals with induced VT, that is, siAT/PC are clearly deviating in their profiles from all other samples.

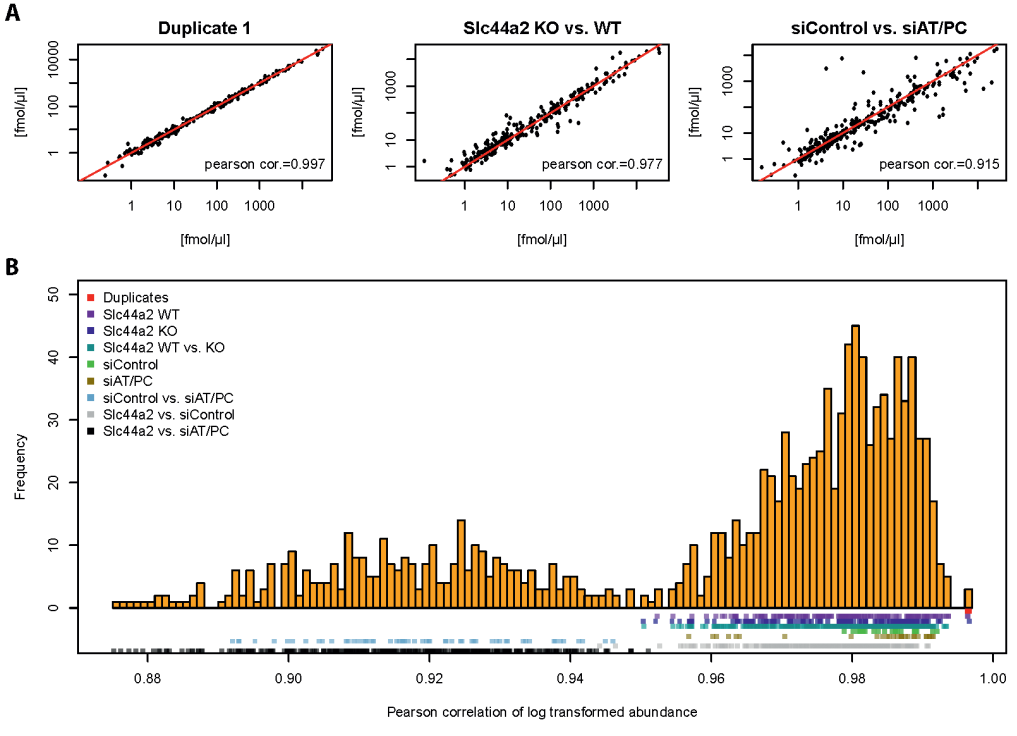

Figure 2. Correlation between samples. N=16 for *Slc44a2+/+* (eight males and eight females), N=15 for *Slc44a2-/-* (six males and eight females), N=8 for siAT/PC, and N=7 for siControl. **(A)** Pairwise correlation between duplicate samples (Duplicate 1), *Slc44a2-/-* and *Slc44a2+/+* (Slc44a2 KO vs. WT), as well as samples from induced VT using siRNA targeting antithrombin and protein C and corresponding controls (siControl vs. siAT/PC) **(B)** Histogram of correlation coefficient values of all pairwise comparisons of samples based on determined protein abundances. PC, protein C; AT, antithrombin; siRNA, small interfering RNA; WT, wild-type; KO, knockout.

Traceable protein changes due to induced venous thrombosis

A clear distinction could be observed between mice treated with siAT/PC, which developed VT, and the siControl treated mice (Figure 2 and Figure S2). Despite developing VT, siAT/PC treated mice remained lively and did not appear sick (i.e. lethargic, unresponsive to stimuli, or hypothermic as may be observed upon progression of the phenotype (31)), nevertheless changes in the plasma proteome appear considerable. The top 10 discriminating plasma proteins are shown in Figure 3A and listed in Table 1A. Principle component analysis (PCA) on these 10 proteins shows a very good separation with principle component (PC) 1 explaining 82% of the variance observed between the two experimental groups (Figure 3E). The log_2 fold changes (log_2 FC) in protein levels also show that the effect on the proteome is substantial with several proteins having more than three times log_2 FC (Figure S3A). As expected antithrombin III is in the list of discriminating proteins with large fold change (log_2 FC of -4.93) which reflects the successful antithrombin gene silencing strategy (Figure 1D). Lower levels of protein C are also expected (32) and were readily observed (log_2 FC of -1.98), although not amongst the top 10 selected most discriminatory proteins. Plasma hemoglobin subunit beta-1 is discriminating and is strongly reduced with log_2 FC of -2.88 upon VT, which is in line with the observed decrease in two other hemoglobulin subunits i.e. alpha and zeta (log_2 FC of -3.94 and -3.97 respectively, Figure S3A).In addition, a strong increase of hemoglobin-binding protein haptoglobin (log_2 FC of 9.20, Figure S3A) is observed. Together these alterations in plasma proteins point toward changes in erythrocyte functioning, which can be explained as erythrocyte trapping and extravasation in the (large veins of the) heads of affected mice is a key feature of this VT model (Figure 1B). Since formation of fibrin-networks (trapping the erythrocytes) is also part of the pathology in this VT model, the decrease in coagulation factor XIIIB (log_2 FC of -1.25) and coagulation factor XIIIA (log_2 FC of -1.91), the two subunits of coagulation factor XIII (FXIII) that is involved in covalent crosslinking of fibrin, is not unexpected either. While consumption of plasma coagulation factors is reported previously in this model (31), this is not supported by the observations in the present study as changes for other coagulation proteins that were included in the current analysis (fibrinogen, coagulation factor II, V, VII, X, XI, XII) were limited (log_2 FC did not exceed -1 or 1). It is important to note that in Safdar et al. (31), the sampling time point is different, i.e. prolonged VT in Safdar et al. versus onset of VT in this study, and the sample collection and handling is different, i.e. normal collection of citrated versus immediate cooling of K_2EDTA plasma which affect the intrinsic proteases activities.

Several proteins among the 10 most discriminating proteins with higher abundance upon VT and number are known as acute phase proteins (APPs) i.e. c-reactive protein (log_2 FC of 1.30), ceruloplasmin (0.80), fibronectin (1.34), alpha-1-acid glycoprotein 2 (3.76), complement C3 (1.01) and complement C8 gamma chain (0.69; (43-45). Various other proteins that increase in their average abundance (Figure S3A), but are not among the top discriminating proteins due to their variance, are also APPs which include serum amyloids (SA) SAa2 (log_2 FC of 11.55), SAa1 (8.91), SAa4 (1.78) and SAp (7.42). Apolipoprotein D was also observed to have a higher abundance in mice with VT (log_2 FC of 0.72), it has however no known role in erythrocyte

function, coagulation, or as an APP. Apolipoprotein D changes upon VT did not coincide with changes in levels of other apolipoproteins included in the analysis (apolipoproteins A-I, A-II, B, C-I, C-II, C-III, C-IV and E).

Plasma proteome influenced by sex group

The (dis)similarities in protein abundance profile according to intervention (Figure 2) as well as the traceable protein changes due to induced VT (Figure S2), demonstrate the capability of the method in capturing protein signatures in experimental VT models. Figure S2 shows further how unsupervised clustering on all data and samples results in perfect discrimination between male and female. We further compared the plasma levels of the wild type (*Slc44a2+/+)* males and females with Figure 3B as well as Table 1 listing the top discriminatory proteins. The $\log_2$ fold changes in plasma protein levels for sex are smaller than those observed upon VT (Figure S3B) and shows that sex has a substantial but more limited impact on the plasma proteome as compared with induced VT. Of note, the protein levels changing mostly do not overlap with the top discriminating proteins for sex. Principal component analysis on the 10 most discriminating proteins shows perfect separation along PC1, which explains 88% of the variance (Figure 3F).

The discriminating proteins are from multiple pathways and include coagulation proteases (vitamin K dependent protein C, $\log_2$ FC of 0.82 and carboxypeptidase B2, $\log_2$ FC of 0.45, a complement protease (C8 alpha and gamma chain, $\log_2$ FC of 2.05 and 1.92 respectively), a protease inhibitor (alpha-1-antitrypsin 1-1, $\log_2$ FC of 4.06), a hormone binding protein (corticosteroid-binding globulin protein, $\log_2$ FC of -1.10), three signaling proteins (adiponectin, $\log_2$ FC of -0.90, epidermal growth factor receptor, $\log_2$ FC of 1.18, interleukin-1 receptor accessory protein, $\log_2$ FC of 0.65) and an immunity-related protein (H-2 class I histocompatibility antigen Q10 alpha chain, $\log_2$ FC of 0.85). For adiponectin and complement C8, an impact of sex on plasma levels was previously reported (46, 47). This observed strong discrimination between the protein profiles of male and female shows that the plasma proteomes for the sexes are different. Subsequently, we performed the analysis of the effect of *Slc44a2* deficiency on the plasma protein levels per sex separately as the anticipated effects of *Slc44a2* deficiency may be more limited.

Table 1. Top 10 discriminating proteins between mice that developed venous thrombosis following injection of small interfering RNA targeting antithrombin and protein C and their controls (siControl) between wild-type male and female mice, and between Slc44a2 -/- (KO) and Slc44a2 +/+ (WT) in male and female mice

					Protein abundancy mean[range] (fmol/µl)					
	Protein names	**Gene names**	**UniprotKB**	**Peptide Sequence**	**siControl**	**siAT/PC**	**WT male**	**WT female**	**KO male**	**KO female**
Top 10 discriminators between siAT/PC and siControl	Alpha-1-acid glycoprotein 2	*Orm2*	P07361	IFADLIVLK	178 [82.2-378]	2410 [1550-4700]	31,1 [13.9-102]	43,7 [27.5-111]	39 [23.8-50.5]	56,3 [29.1-169]
	Antithrombin-III	*Serpinc1*	P32261	DDLYVSDAFHK	851 [588-1090]	27,8 [16.1-45.1]	1040 [725-1440]	1160 [1030-1400]	1100 [782-1240]	1100 [963-1270]
	Apolipoprotein D	*Apod*	P51910	IPASFEK	35 [24.7-38.6]	57,6 [44.4-75]	37,5 [22.6-47.4]	41 [33.7-48.6]	36,8 [17.4-47.8]	46,1 [41.3-52.2]
	Ceruloplasmin	*Cp*	Q61147	DIFTGLIGPMK	340 [269-408]	591 [465-785]	419 [363-504]	448 [398-525]	447 [395-503]	442 [383-516]
	Coagulation factor XIII A chain	*F13a1*	Q8BH61	FQEGQEEER	89,3 [65.8-107]	23,8 [3.87-52.1]	97,8 [73.9-116]	118 [54.9-164]	109 [81.8-164]	87,3 [67.3-141]
	Complement C3	*C3*	P01027	GTLSVVAVYHAK	1240 [896-1710]	2490 [1760-3220]	1170 [923-1360]	1610 [1260-1960]	1210 [1100-1290]	1880 [838-3780]
	Complement component C8 gamma chain	*C8g*	Q8VCG4	FLFQVSR	119 [86.5-153]	192 [167-224]	405 [302-518]	108 [58.3-163]	397 [321-561]	105 [61.4-185]
	C-reactive protein	*Crp Ptx1*	P14847	AFVFPK	59,3 [51.4-68.5]	146 [109-174]	77,9 [59.3-109]	80,3 [61.7-104]	75,5 [53.6-104]	79,3 [64.5-103]
	Fibronectin	*Fn1*	P11276	SYTITGLQPGTDYK	398 [306-519]	1010 [622-1140]	469 [377-588]	548 [380-663]	464 [402-517]	521 [421-632]
	Hemoglobin subunit beta-1	*Hbb-b1*	P02088	VITAFNDGLNHLDSLK	6260 [2930-9130]	853 [422-1540]	4900 [2640-9160]	5290 [3870-7100]	3740 [1170-6610]	4800 [2860-8410]

Table 1 (continued). Top 10 discriminating proteins between mice that developed venous thrombosis following injection of small interfering RNA targeting antithrombin and protein C and their controls (siControl) between wild-type male and female mice, and between Slc44a2 / (KO) and Slc44a2 þ/þ (WT) in male and female mice

	Protein names	Gene names	UniprotKB	Peptide Sequence	Protein abundancy mean[range] (fmol/µl)					
					siControl	siAT/PC	WT male	WT female	KO male	KO female
Top 10 discriminators between female and male in WT	Adiponectin	*Adipoq*	Q60994	SAFSVGLETR	25,3 [16.8-37.7]	18,1 [13-25.3]	16 [12.9-20.1]	29,9 [24.5-37.3]	17,5 [12.2-24.6]	27,2 [20.7-36.4]
	Alpha-1-antitrypsin 1-1	*Serpina1a*	P07758	VINDFVEK	7100 [5400-9700]	6460 [4610-8400]	15400 [13400-18300]	8820 [6850-11000]	15300 [12800-19100]	9170 [7010-11800]
	Carboxypeptidase B2	*Cpb2*	Q9JHH6	YGFLLPER	62,9 [49-84.2]	89,9 [51.9-130]	99,3 [81.9-114]	72,7 [63.2-81.6]	101 [78.8-118]	76,4 [67.8-88.7]
	Complement component C8 beta chain	*C8b*	Q8BH35	GGTSEDITALAYK	129 [90.6-164]	220 [156-299]	478 [415-640]	128 [76.6-185]	516 [391-799]	133 [78.8-246]
	Complement component C8 gamma chain	*C8g*	Q8VCG4	FLFQVSR	119 [86.5-153]	192 [167-224]	405 [302-518]	108 [58.3-163]	397 [321-561]	105 [61.4-185]
	Corticosteroid-binding globulin	*Serpina6*	Q06770	DTPLTLTVLHK	1030 [729-1340]	647 [403-879]	653 [462-1040]	1400 [1240-1490]	819 [394-1090]	1550 [883-2140]
	Epidermal growth factor receptor	*Egfr*	Q01279	IPLENLQIIR	16,8 [11.3-21.4]	28,8 [20.2-46.4]	44,3 [29.2-57.2]	19,6 [10.5-24.5]	37,4 [14.8-52.5]	18,1 [11.1-33.3]
	H-2 class I histocompatibility antigen, Q10 alpha chain	*H2-Q10*	P01898	YFETSVSRPGLGEPR	292 [217-421]	256 [180-331]	623 [458-837]	345 [281-442]	677 [538-973]	374 [326-421]
	Interleukin-1 receptor accessory protein	*Il1rap*	Q61730	VAFPLEVVQK	136 [103-184]	115 [79.3-143]	263 [212-305]	167 [148-185]	258 [195-313]	164 [126-194]
	Vitamin K-dependent protein C	*Proc*	P33587	LGEYDLR	19,2 [14.3-23.5]	4,88 [2.26-7]	38,2 [32.4-45.6]	21,7 [16.8-31.5]	34,8 [25.4-38]	24,1 [19.8-32.7]

Table 1 (continued). Top 10 discriminating proteins between mice that developed venous thrombosis following injection of small interfering RNA targeting antithrombin and protein C and their controls (siControl) between wild-type male and female mice, and between Slc44a2 / (KO) and Slc44a2 þ/þ (WT) in male and female mice

	Protein names	Gene names	UniprotKB	Peptide Sequence	Protein abundancy mean[range] (fmol/µl)					
					siControl	siAT/PC	WT male	WT female	KO male	KO female
Top 10 discriminators between WT and Slc44a2 KO in female	Glycosylation-dependent cell adhesion molecule 1	*Glycam1*	Q02596	DNVVIESTKPENQEAQDGLR	5,14 [2.1-8.32]	4,76 [3.36-8.13]	0,278 [0-0.731]	5,28 [4.37-7.48]	0,666 [0.521-0.944]	8,46 [5.7-11.5]
	Interleukin-18-binding protein	*Il18bp*	Q9Z0M9	ALVLEELSPTLR	5,07 [3.71-6.57]	7,68 [5.76-9.71]	4,98 [3.8-6.96]	5,87 [5.31-6.58]	6,95 [4.61-9.85]	6,93 [6.36-7.85]
	Macrophage colony-stimulating factor 1 receptor	*Csf1r*	P09581	LEIPLNSDFQDNYYK	37,7 [30.7-51.5]	26,5 [18.1-34.4]	39,1 [31.2-50.4]	44,5 [37.6-52.7]	50,2 [37.4-73.5]	49,3 [45.6-53.5]
	Uteroglobin	*Scgb1a1*	Q06318	LVDTLPQETR	5,98 [4.47-8.58]	15,2 [5.87-50]	10,6 [6.98-15.2]	10,9 [7.63-14.9]	9,03 [7.11-12.7]	7,74 [4.76-11.2]
	Thrombospondin-1	*Thbs1*	P35441	FVFGTTPEDILR	4,5 [4.29-4.77]	4,67 [4.35-5.17]	4,84 [4.64-4.98]	5,96 [4.33-13.4]	4,56 [4.4-4.84]	4,5 [4.31-4.82]
	Ubiquitin-like protein ISG15	*Isg15*	Q64339	IGVPAFQQR	16,4 [8.44-23.6]	6,59 [3.64-13]	11,3 [6.94-18.3]	13,6 [9.1-18.4]	15,6 [8.07-22.3]	21,2 [13.9-40.8]
	Collagen alpha-1(XII) chain	*Col12a1*	Q60847	TPDEEFK	8,43 [0-11.6]	8,33 [0-11.8]	11,3 [0-14.9]	7,85 [0-11.3]	7,58 [0-11.9]	11,4 [9.71-14.9]
	Plasma kallikrein	*Klkb1*	P26262	TGAISGHSLK	55 [42.7-70.4]	39,5 [26.5-49.3]	86,8 [72.3-99.7]	68,1 [62.1-81.7]	77,2 [57.7-95.5]	60,5 [52.6-72.3]
	Complement factor H	*Cfh*	P06909	VEYSHGEVVK	10,2 [7.07-14.2]	18 [12.3-23.1]	13,2 [10.1-18.1]	11,7 [8.23-15.7]	13,6 [10.2-16.6]	14,1 [10.9-17.5]
	Ig gamma-3 chain C region	*Ighg3*	P03987	ALPAPIER	300 [9.19-491]	266 [162-373]	838 [452-1670]	1380 [212-3110]	636 [330-819]	660 [334-896]

Table 1 (continued). Top 10 discriminating proteins between mice that developed venous thrombosis following injection of small interfering RNA targeting antithrombin and protein C and their controls (siControl) between wild-type male and female mice, and between Slc44a2 / (KO) and Slc44a2 þ/þ (WT) in male and female mice

					Protein abundancy mean[range] (fmol/µl)					
	Protein names	**Gene names**	**UniprotKB**	**Peptide Sequence**	**siControl**	**siAT/PC**	**WT male**	**WT female**	**KO male**	**KO female**
Top 10 discriminators between WT and Slc44a2 KO in male	Intercellular adhesion molecule 1	*Icam1*	P13597	GEEILSR	5,87 [4.07-8.25]	7,34 [5.8-10.7]	6,87 [5.27-7.38]	8,22 [7.01-9.03]	8,59 [7.27-9.96]	8,58 [6.77-10.2]
	Glycosylation-dependent cell adhesion molecule 1	*Glycam1*	Q02596	DNVVIESTKPENQEAQDGLR	5,14 [2.1-8.32]	4,76 [3.36-8.13]	0,278 [0-0.731]	5,28 [4.37-7.48]	0,666 [0.521-0.944]	8,46 [5.7-11.5]
	Thrombospondin-1	*Thbs1*	P35441	FVFGTTPEDILR	4,5 [4.29-4.77]	4,67 [4.35-5.17]	4,84 [4.64-4.98]	5,96 [4.33-13.4]	4,56 [4.4-4.84]	4,5 [4.31-4.82]
	Apolipoprotein A-IV	*Apoa4*	P06728	SLEDLNR	2050 [1510-3000]	1800 [1480-2550]	2540 [2260-3150]	2320 [2010-2970]	3060 [2730-3420]	2340 [2040-2690]
	Complement C1s-A subcomponent	*C1sa*	Q8CG14	TTLLENAQR	53,9 [38.8-70.5]	56,1 [43.1-79]	80,7 [69.8-93.3]	57,5 [44-64.9]	68,8 [53-77.6]	64,1 [35.8-80.9]
	Retinoic acid receptor responder protein 2	*Rarres2*	Q9DD06	SLQVALEEFHK	2,27 [1.72-2.79]	1,8 [0-2.61]	3,03 [2.38-4]	2,32 [1.93-3.3]	2,46 [2.19-2.88]	2,59 [1.54-3.33]
	Alpha-1-acid glycoprotein 2	*Orm2*	P07361	IFADLIVLK	178 [82.2-378]	2410 [1550-4700]	31,1 [13.9-102]	43,7 [27.5-111]	39 [23.8-50.5]	56,3 [29.1-169]
	Histidine-rich glycoprotein	*Hrg*	Q9ESB3	FESEFPQISK	340 [251-471]	584 [370-886]	448 [398-535]	407 [274-484]	524 [438-620]	453 [328-575]
	Kunitz-type protease inhibitor 1	*Spint1*	Q9R097	YTSGFDELQNIHFLSDK	3,59 [1.87-4.58]	5,16 [4.27-6.5]	4,61 [3.44-6.42]	4,29 [3.42-5.77]	3,4 [1.63-4.5]	3,85 [2.85-5.23]
	Prenylcysteine oxidase	*Pcyox1*	Q9CQF9	YQSHDYAFSSVEK	4,34 [0-7.73]	5,81 [0-9.22]	7,33 [6.19-8.65]	5,57 [0-7.73]	8,41 [7.17-9.78]	5,64 [0-9.52]

Abbreviations: KO, knockout; PC, protein C; WT, wild type; siRNA, small interfering RNA.

Effect of Slc44a2 on plasma proteome is limited

No obvious discrimination between *Slc44a2-/-* and *Slc44a2*+/+ mice was observed when all proteins were included in the clustering (Figure S2). However, limiting the analysis to the top 10 discriminating proteins between these groups (Table 1), right grouping in Slc44a2-/- and +/+ during cluster analysis for males (Figure 3C) as well as for females (Figure 3D) can be obtained with a single *Slc44a2*+/+ female outlier. PCA on these discriminatory proteins explains 44.6 and 46.2% of variance in male (Figure 3G) and female (Figure 3H), respectively. This is lower compared with the previous PCAs of the VT model as well as the discrimination between female and male. Also, the fold changes in protein levels for *Slc44a2* deficiency are smaller compared with those of VT and sex groups (Figure S3C and S3D). As observed for the male versus female comparison, for *Slc44a2* mice there is no overlap between the proteins that change most in abundance and the proteins that discriminate most for *Slc44a2* status, both in females and males.

The discriminating proteins are from multiple pathways and interestingly, thrombospondin-1 (Tsp-1) and glycosylation-dependent cell adhesion molecule-1 (Glycam-1) are present in the top 10 of both sexes. Tsp-1 is low abundant (Table 1) in plasma and only modestly reduced in plasma of *Slc44a2-/-* as compared to *Slc44a2*+/+ mice (for male and female $\log_2$ FC of -0.09 and -0.41 respectively). This protein functions in platelet signaling and its deficiency was shown to lead to decreased (arterial) thrombus formation in mice (48, 49). Signature protein Glycam-1 is higher in abundancy in *Slc44a2-/-* as compared to *Slc44a2*+/+ mice (Figure S3B, $\log_2$ FC male: 1.26 and female: 0.68). Little is known about the biological function of Glycam-1, though it was shown to be a ligand for L-selectin, expressed on endothelial cells and involved in neutrophil rolling in inflammation (50, 51). In summary, *Slc44a2* deficiency has a smaller impact on the plasma proteome compared to VT and sex, nevertheless we were able to establish a plasma proteome signature for *Slc44a2* for both male and female mice.

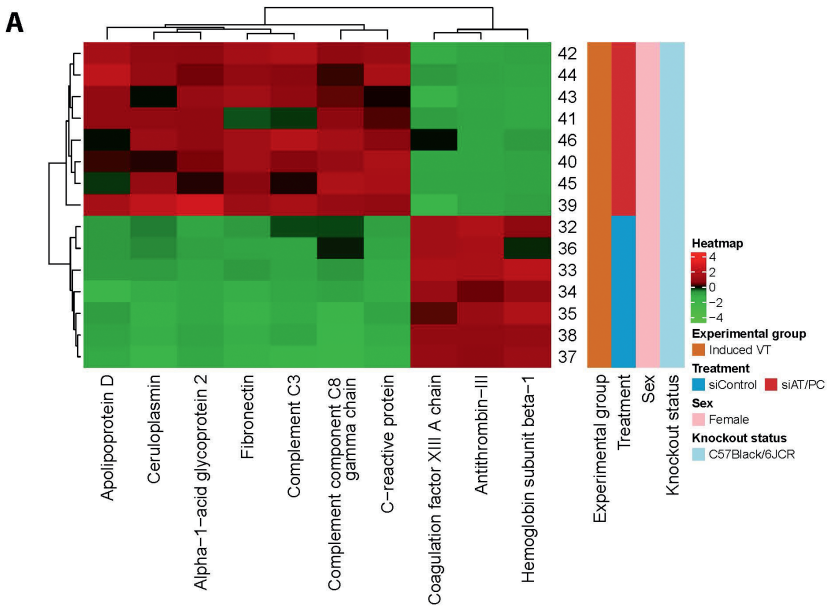
A
42
44
43
41
46
40
45
39
32
36
33
34
35
38
37
Heatmap
4
2
0
−2
−4
Experimental group
Induced VT
Treatment
siControl
siAT/PC
Sex
Female
Knockout status
C57Black/6JCR
Apolipoprotein D
Ceruloplasmin
Alpha−1−acid glycoprotein 2
Fibronectin
Complement C3
Complement component C8 gamma chain
C−reactive protein
Coagulation factor XIII A chain
Antithrombin−III
Hemoglobin subunit beta−1
Experimental group
Treatment
Sex
Knockout status

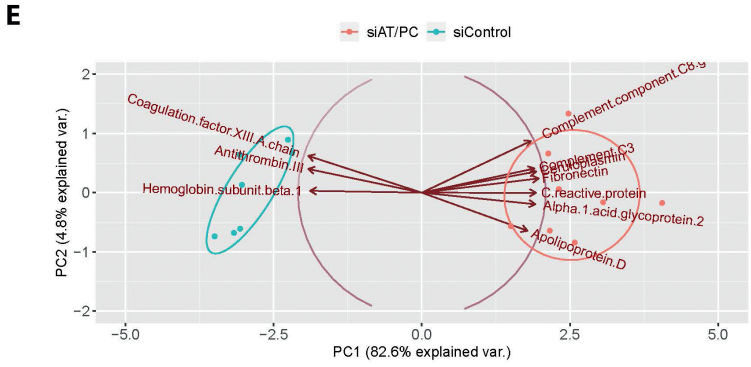
E
siAT/PC
siControl
Coagulation.factor.XIII.A.chain
Antithrombin.III
Hemoglobin.subunit.beta.1
Complement.component.C8.g
Complement.C3
Ceruloplasmin
Fibronectin
C.reactive.protein
Alpha.1.acid.glycoprotein.2
Apolipoprotein.D
PC2 (4.8% explained var.)
PC1 (82.6% explained var.)
2
1
0
−1
−2
−5.0
−2.5
0.0
2.5
5.0

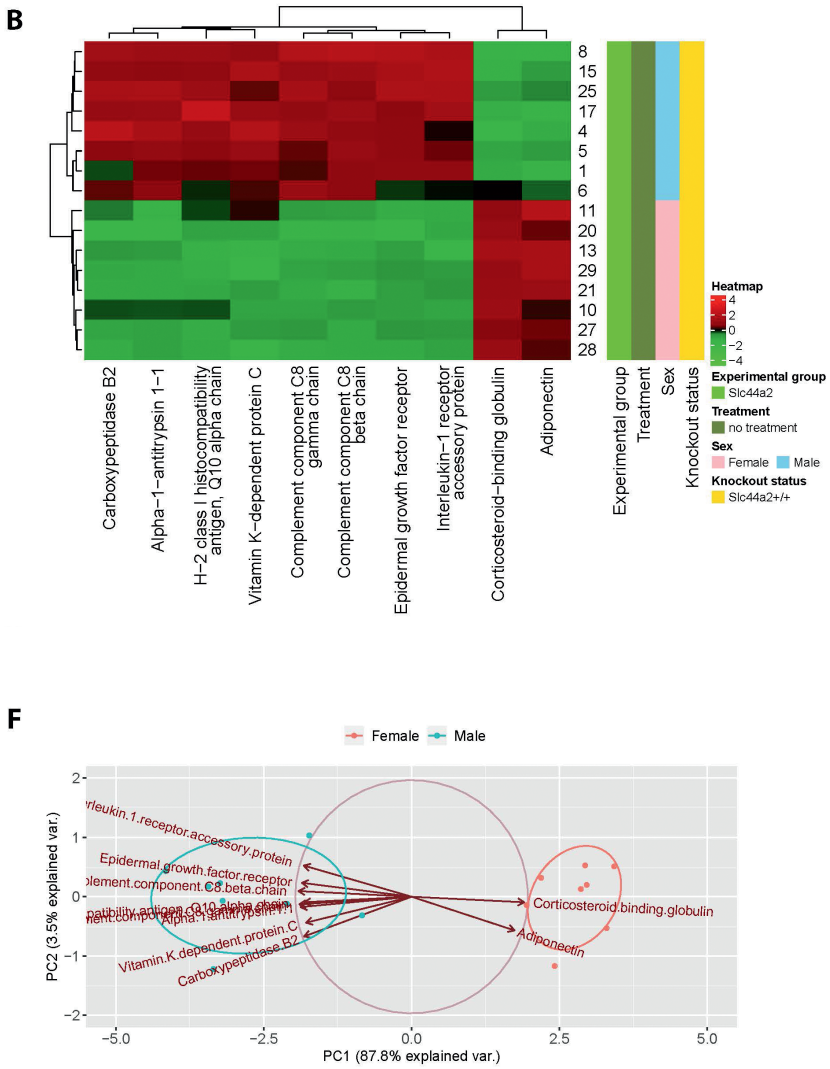

Figure 3. Discrimination between the various study groups based on the plasma abundance of the selected top 10 discriminating proteins in each group (Table 1). Discriminations are illustrated using hieratical clustering and heatmaps **(A-D)** as well as corresponding principle component analysis **(E-H)**. N=8 for female wild-type mice (*Slc44a2*+/+), N=8 for female *Slc44a2* deficient mice (*Slc44a2*-/-), N=8 for male *Slc44a2*+/+, N=6 for male *Slc44a2*-/-, N=8 for siRNA targeting antithrombin and protein C (siAT/PC), and N=7 for siControl. **(A)** and **(E)** show the results for siAT/PC treated mice and their controls (siControl). **(B)** and **(F)** show the discrimination between the wild type male and female mice.

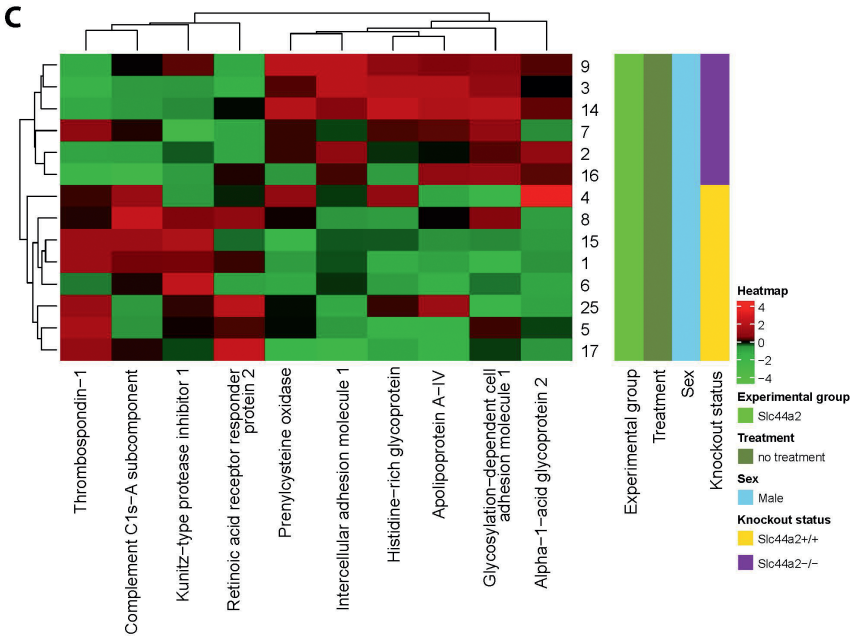
C
9
3
14
7
2
16
4
8
15
1
6
25
5
17
Thrombospondin−1
Complement C1s−A subcomponent
Kunitz−type protease inhibitor 1
Retinoic acid receptor responder protein 2
Prenylcysteine oxidase
Intercellular adhesion molecule 1
Histidine−rich glycoprotein
Apolipoprotein A−IV
Glycosylation−dependent cell adhesion molecule 1
Alpha−1−acid glycoprotein 2
Experimental group
Treatment
Sex
Knockout status
Heatmap
4
2
0
−2
−4
Experimental group
Slc44a2
Treatment
no treatment
Sex
Male
Knockout status
Slc44a2+/+
Slc44a2−/−

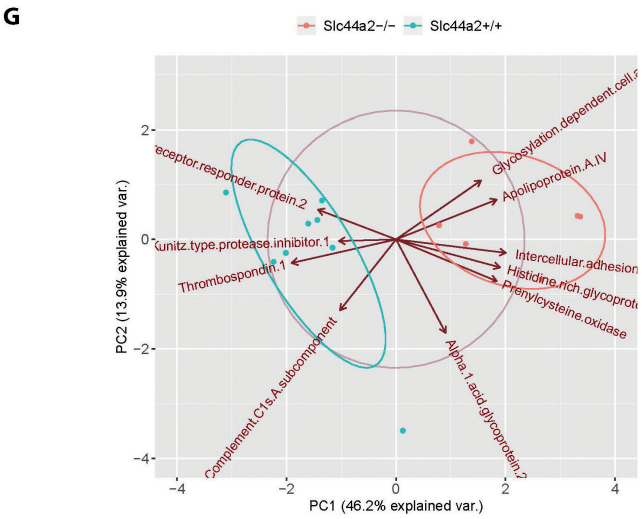
G
Slc44a2−/−
Slc44a2+/+
Glycosylation.dependent.cell.a
Apolipoprotein.A.IV
Intercellular.adhesion
Histidine.rich.glycoprote
Prenylcysteine.oxidase
Alpha.1.acid.glycoprotein.2
Complement.C1s.A.subcomponent
Thrombospondin.1
unitz.type.protease.inhibitor.1
eceptor.responder.protein.2
PC2 (13.9% explained var.)
PC1 (46.2% explained var.)
2
0
−2
−4
−4
−2
0
2
4

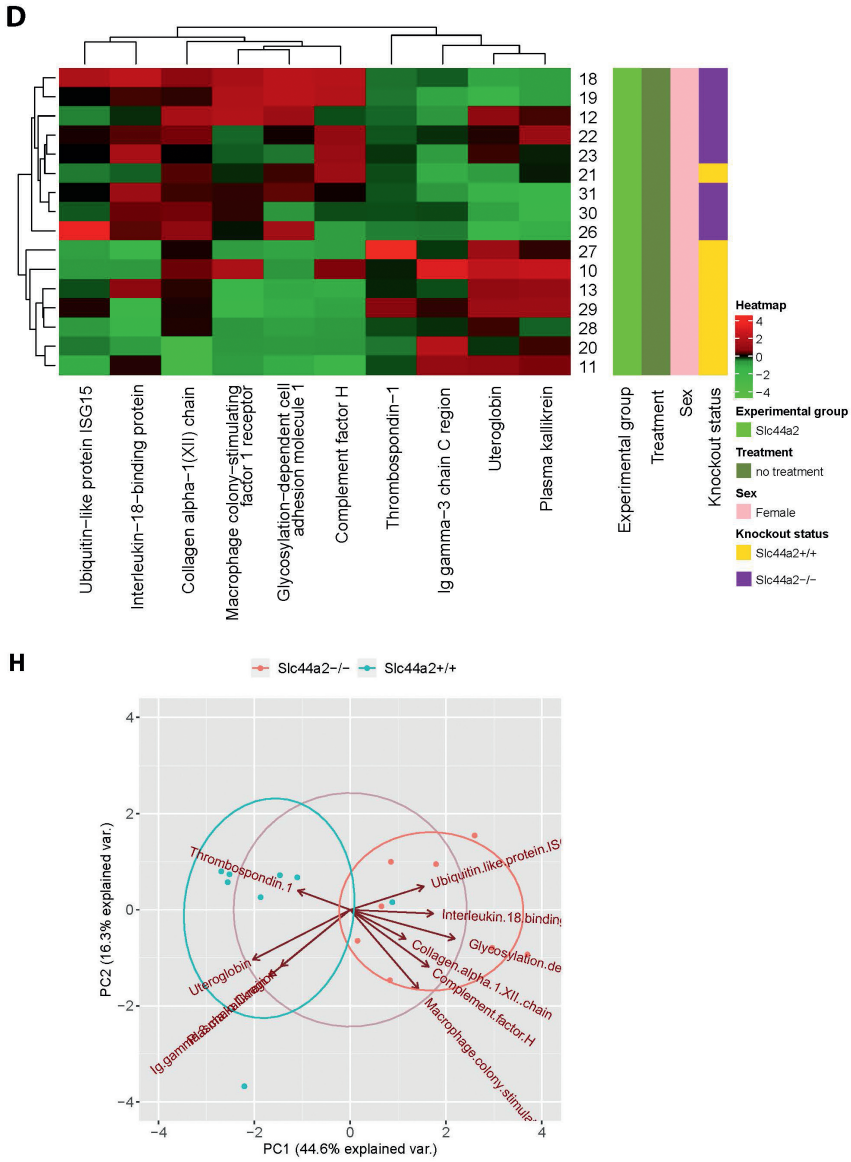

Figure 3 (continued). Discrimination between the various study groups based on the plasma abundance of the selected top 10 discriminating proteins in each group (Table 1). Discriminations are illustrated using hieratical clustering and heatmaps **(A-D)** as well as corresponding principle component analysis **(E-H)**. N=8 for female wild-type mice (*Slc44a2+/+*), N=8 for female *Slc44a2* deficient mice (*Slc44a2-/-*), N=8 for male *Slc44a2+/+*, N=6 for male *Slc44a2-/-*, N=8 for siRNA targeting antithrombin and protein C (siAT/PC), and N=7 for siControl. **(C)** and **(G)**, as well as **(D)** and **(H)** show the discrimination between *Slc44a2+/+* and *Slc44a2-/-* in male and female respectively. PC, protein C; AT, antithrombin; siRNA, small interfering RNA.

Discussion

We investigated the possible plasma protein signatures in mice following the onset of VT and in mice lacking Slc44a2 which was recently characterized as a VT-susceptibility gene in human GWAS. We used 375 validated multiplexed MS-based protein assays to measure the plasma protein levels. The mouse model where VT follows RNA interference mediated silencing of antithrombin and protein C was included as it features a strong VT phenotype, coinciding with strong clinical signs. Upon VT numerous plasma proteins changed yielding a strong protein signature that was easily measurable using our method. Furthermore, profile (dis)similarities according to intervention demonstrated the capability of the method in capturing plasma protein dynamic. In mice lacking *Slc44a2,* the protein signatures were primarily overruled by the differences between male and female and not the absent gene. By looking in each group separately, modest alteration of two proteins was identified in males and females lacking *Slc44a2*. This indicates that the link between SLC44A2 and VT is outside traditional coagulation- and fibrinolysis-related pathways. Possibly, SLC44A2 affects (blood) cell-cell interactions as reflected Glycam1 and L-selectin being part of gene signature.

In addition to serving as validation experiment, the strong signature obtained for the mouse VT model also provided novel insights into this model. The presence of APPs (haptoglobin, fibrinogen, c-reactive protein, ceruloplasmin, fibronectin, alpha-1-acid glycoprotein 2, complement C3, complement C8, SAa2, SAa1, SAa4 and SAp) among the signature for VT indicate that the VT following silencing of natural anticoagulants has a more systemic and acute impact than currently known. The microscopically visible VT is confined to the large veins of the head is characterized among others by a strong recruitment and influx of leukocytes (32). Whether the local recruitment of leukocytes is causing the systemic acute phase response or this is a secondary effect is subject to speculation. Apart from leukocytes, another major constituent of the thrombi in the large veins of the head is trapped and recruited erythrocytes (32). In addition, erythrocytes extravasate upon rupture of the occluded veins. Circulating hemoglobulin and haptoglobin levels (inversely) relate to blood erythrocyte numbers, and may explain why the plasma levels change when erythrocyte-rich thrombi are formed in the head. We expected that the coagulation factors, which were included in the assay, should be among the signature proteins for VT as these may drop in circulating levels being consumed at the expense of thrombus formation. Coagulation factor XIII (FXIII, both FXIIIa and FXIIIb subunits) is the only coagulation protein among the top 10 discriminatory proteins for VT. FXIII is a well-known contributor to fibrin network formation and stabilization (52). In addition, Factor XIII is involved in (fibrin-mediated) erythrocyte retention in venous thrombi (53, 54). The drop in plasma FXIII levels possibly reflects trapping of the FXIII protein in the fibrin-network of the formed thrombi. Hence, it would be interesting to determine the (critical) role of this protein in this model of VT for example by subjecting FXIII knockout mice to the model.

Although the impact of sex overruled the effect *Slc44a2*, we obtained a specific *Slc44a2* signature focusing on most discriminating proteins The proteins involved in these sex-specific signatures have not yet been subject to investigation with respect to control by sex hormones (estrogens and testosterone). Hence, whether these strong male-female differences are a direct result of regulation, or an indirect effect caused by for example differences in body weight, plasma volume, organ size and function can only be speculated. A recent study aimed at determining plasma proteome dynamics in different laboratory mouse strains including C57BL/6J (26) found complement C8 gamma and beta chain, Epidermal growth factor receptor and corticosteroid-binding globulin among the plasma proteins that discriminated males from females, which is in line with our findings using mice of the same background. In a mouse study focusing on sex specific liver gene expression epidermal growth factor receptor and complement factor 8 were found to be different between males and females for liver transcript also in line with our findings in plasma (55). Future studies into the origin of the strong sex-specific plasma protein signature are of interest. For the present study, sex is a major determinant of the plasma proteome and therefore males and females should essentially be considered as two different groups.

Slc44a2 deficient mice appear normal and so far impact on disease (hearing loss, VT) only became apparent upon challenges (13, 14). Hence, the very modest impact of *Slc44a2* deficiency on the plasma proteome supports the concept that SLC44A2 has a limited role in normal physiology, or one that can be compensated for. In the top 10 discriminating proteins for *Slc44a2* two proteins were present in both females and males, i.e. Tsp-1 and Glycam-1. Tsp-1 plasma abundance was lower in *Slc44a2* deficient mice. Tsp-1 is an adhesive glycoprotein that mediates cell-to-cell and cell-to-matrix interactions, first identified as a component of the secreted product of activated platelets (56). Tsp-1 was previously linked to thrombosis, as its absence delays thrombus formation in mice (48, 49). Part of these Tsp-1 effects require interaction with VWF. SLC44A2 also interacts with VWF (12) and we observed a modest decrease in VWF abundance in *Slc44a2* deficient mice before (14). For future studies on the role of SLC44A2 in VT and its possible interaction with VWF it is recommended to investigate Tsp-1. Glycam-1 abundance was higher in Slc44a2 deficient mice. Glycam-1 has not been linked to thrombosis before, it was however shown to be a ligand for L-selectin, expressed on endothelial cells, and involved in neutrophil rolling in inflammation (50, 51). In general, selectins (including also P- and E-selectins) are important in mediating interactions between leukocytes and the vessel wall and P- and E-selectin are well-known player in thrombosis. In future studies on SLC44A2, it is worthwhile to investigate possible roles of Glycam1 and L-selectin. In summary no major effect of *Slc44a2* deficiency in plasma was found. The minimal effect observed involves changes in Glycam-1 and tsp-1 plasma levels, which suggest a mechanism related to cell-cell interactions. Observations regarding the role of SLC44A2 in experimental VT in mice (unpublished work) showed that *Slc44a2* deficiency does not influence VT driven by hypercoagulability (31, 32). *Slc44a2* deficient mice do however display reduced thrombus formation following flow restriction (57) where inflammatory cells from the blood, including neutrophils and platelets, are important

contributors (58, 59). Moreover, it was recently demonstrated that platelets primed by VWF display activated integrin $\alpha_{IIb}\beta_3$ (but not CD62P), which can then bind neutrophil SLC44A2 and mediate NETosis under venous flow (60), suggesting that SLC44A2 is a mediator of cell-cell interactions. Therefore, we suggest incorporating the cellular compartment of the blood in further investigation of the effect of SLC44A2 on VT. To elucidate the contribution of SLC44A2 on the different cell types, cell specific knockouts of *Slc44a2* might be interesting to include.

A strength of MS-based targeted proteomics assays is specificity. Each assay is designed to target a specific peptide with multi-level of assurance. However, the measured endogenous peptide can also be originated from degradation products or inactive forms of the protein. It is possible to design an experiment with multiple peptides per proteins (28) to infer information on the level of protein (in)activity; however, this was not considered in the current study. Nonetheless, quantitative-targeted proteomics allowed detecting subtle changes in abundance of plasma proteins in murine VT research for which currently no traditional (antibody-based) assays are available. Besides unspecificity, the antibody assays that are available for mouse require substantial amounts of plasma making measurement of multiple protein levels from one sample not feasible. For example, when we examined available Tsp-1 antibody assay, these required up to 200 µL plasma, which was unavailable from each mouse, compared with less than 10 µl for MS. The high multiplicity and precision allow determining the abundances of hundreds of proteins with standardized sample processing, producing a sharp snapshot of the targeted proteins in the samples. Using simple data analysis method like correlation, hierarchical clustering, and PCA allow generating clear signatures of conditions and protein signatures were generated for a VT model, sex and a *Slc44a2* deficient mice.

Disclosure of Conflicts of Interest

J.T., C.X.M., H.H.V. and B.J.M.V.V. report grants from Trombosestichting Nederland, grants from Landsteiner Foundation for Blood Transfusion Research, during the conduct of the study. C.H.B. reports grants from Genome Canada and Genome British Columbia, during the conduct of the study; personal fees and other from MRM proteomics, nonfinancial support from Creative Molecules, personal fees from Molecular You, outside the submitted work. C.H.B. is the chief strategy officer of MRM Proteomics, Inc. Y.M. reports grants from Genome Canada; Genome British Columbia, during the conduct of the study.

Acknowledgments

The authors thank Thankam S. Nair, Pavan K. Kommareddi, and Thomas E. Carey (University of Michigan, Ann Arbor, MI, USA) for the development and provision of the *Slc44a2* deficient mice.

Author contributions

Experimental design: J.T, B.J.M.v.V., Y.M. Sample collection J.T., B.J.M.v.V. MRM experiments: S.A.M and Y.M. Data analysis and visualization: J.T. and Y.M., results interpretation and first draft of the manuscript J.T., B.J.M.v.V., Y.M. All authors commented on manuscript drafts and contributed to the text.

References

1. Furie B, Furie BC. Mechanisms of thrombus formation. *N Engl J Med*. 2008;359(9):938-49.
2. Rosendaal FR. Venous thrombosis: the role of genes, environment, and behavior. *Hematology Am Soc Hematol Educ Program*. 2005:1-12.
3. Tripodi A. Levels of coagulation factors and venous thromboembolism. *Haematologica*. 2003;88(6):705-11.
4. Rosendaal FR. Causes of venous thrombosis. *Thromb J*. 2016;14(Suppl 1):24.
5. Germain M, Chasman DI, de Haan H, et al. Meta-analysis of 65,734 individuals identifies TSPAN15 and SLC44A2 as two susceptibility loci for venous thromboembolism. *Am J Hum Genet*. 2015;96(4):532-42.
6. Roumen-Klappe EM, den Heijer M, van Uum SH, et al. Inflammatory response in the acute phase of deep vein thrombosis. *J Vasc Surg*. 2002;35(4):701-6.
7. Fox EA, Kahn SR. The relationship between inflammation and venous thrombosis. A systematic review of clinical studies. *Thromb Haemost*. 2005;94(2):362-5.
8. Conway EM. Reincarnation of ancient links between coagulation and complement. *J Thromb Haemost*. 2015;13 Suppl 1:S121-32.
9. Mosevoll KA, Lindas R, Tvedt TH, et al. Altered plasma levels of cytokines, soluble adhesion molecules and matrix metalloproteases in venous thrombosis. *Thromb Res*. 2015;136(1):30-9.
10. Morelli VM, Lijfering WM, Bos MHA, et al. Lipid levels and risk of venous thrombosis: results from the MEGA-study. *Eur J Epidemiol*. 2017;32(8):669-81.
11. Hinds DA, Buil A, Ziemek D, et al. Genome-wide association analysis of self-reported events in 6135 individuals and 252 827 controls identifies 8 loci associated with thrombosis. *Hum Mol Genet*. 2016;25(9):1867-74.
12. Bayat B, Tjahjono Y, Berghofer H, et al. Choline Transporter-Like Protein-2: New von Willebrand Factor-Binding Partner Involved in Antibody-Mediated Neutrophil Activation and Transfusion-Related Acute Lung Injury. *Arterioscler Thromb Vasc Biol*. 2015;35(7):1616-22.
13. Kommareddi P, Nair T, Kakaraparthi BN, et al. Hair Cell Loss, Spiral Ganglion Degeneration, and Progressive Sensorineural Hearing Loss in Mice with Targeted Deletion of Slc44a2/Ctl2. *J Assoc Res Otolaryngol*. 2015;16(6):695-712.
14. Tilburg J, Adili R, Nair TS, et al. Characterization of hemostasis in mice lacking the novel thrombosis susceptibility gene Slc44a2. *Thromb Res*. 2018;171:155-9.
15. Geyer PE, Kulak NA, Pichler G, et al. Plasma Proteome Profiling to Assess Human Health and Disease. *Cell Syst*. 2016;2(3):185-95.
16. Huttenhain R, Choi M, Martin de la Fuente L, et al. A Targeted Mass Spectrometry Strategy for Developing Proteomic Biomarkers: A Case Study of Epithelial Ovarian Cancer. *Mol Cell Proteomics*. 2019;18(9):1836-50.
17. Niu L, Geyer PE, Wewer Albrechtsen NJ, et al. Plasma proteome profiling discovers novel proteins associated with non-alcoholic fatty liver disease. *Mol Syst Biol*. 2019;15(3):e8793.
18. Pimienta G, Heithoff DM, Rosa-Campos A, et al. Plasma Proteome Signature of Sepsis: a Functionally Connected Protein Network. *Proteomics*. 2019;19(5):e1800389.

19. Wewer Albrechtsen NJ, Geyer PE, Doll S, et al. Plasma Proteome Profiling Reveals Dynamics of Inflammatory and Lipid Homeostasis Markers after Roux-En-Y Gastric Bypass Surgery. *Cell Syst*. 2018;7(6):601-12 e3.
20. Terfve C, Sabido E, Wu Y, et al. System-Wide Quantitative Proteomics of the Metabolic Syndrome in Mice: Genotypic and Dietary Effects. *Journal of proteome research*. 2017;16(2):831-41.
21. Liumbruno GM, Franchini M. Proteomic analysis of venous thromboembolism: an update. *Expert Rev Proteomics*. 2013;10(2):179-88.
22. Lippi G, Favaloro EJ, Plebani M. Proteomic analysis of venous thromboembolism. *Expert Rev Proteomics*. 2010;7(2):275-82.
23. Bruzelius M, Iglesias MJ, Hong MG, et al. PDGFB, a new candidate plasma biomarker for venous thromboembolism: results from the VEREMA affinity proteomics study. *Blood*. 2016;128(23):e59-e66.
24. Ganesh SK, Sharma Y, Dayhoff J, et al. Detection of venous thromboembolism by proteomic serum biomarkers. *PLoS One*. 2007;2(6):e544.
25. Stachowicz A, Siudut J, Suski M, et al. Optimization of quantitative proteomic analysis of clots generated from plasma of patients with venous thromboembolism. *Clin Proteomics*. 2017;14:38.
26. Michaud SA, Sinclair NJ, Petrosova H, et al. Molecular phenotyping of laboratory mouse strains using 500 multiple reaction monitoring mass spectrometry plasma assays. *Commun Biol*. 2018;1:78.
27. Ding J, Berryman DE, Jara A, et al. Age- and sex-associated plasma proteomic changes in growth hormone receptor gene-disrupted mice. *J Gerontol A Biol Sci Med Sci*. 2012;67(8):830-40.
28. Mohammed Y, van Vlijmen BJ, Yang J, et al. Multiplexed targeted proteomic assay to assess coagulation factor concentrations and thrombosis-associated cancer. *Blood Adv*. 2017;1(15):1080-7.
29. Mohammed Y, Pan J, Zhang S, et al. ExSTA: External Standard Addition Method for Accurate High-Throughput Quantitation in Targeted Proteomics Experiments. *Proteomics Clin Appl*. 2018;12(2).
30. Addona TA, Abbatiello SE, Schilling B, et al. Multi-site assessment of the precision and reproducibility of multiple reaction monitoring-based measurements of proteins in plasma. *Nat Biotechnol*. 2009;27(7):633-41.
31. Safdar H, Cheung KL, Salvatori D, et al. Acute and severe coagulopathy in adult mice following silencing of hepatic antithrombin and protein C production. *Blood*. 2013;121(21):4413-6.
32. Heestermans M, Salloum-Asfar S, Streef T, et al. Mouse venous thrombosis upon silencing of anticoagulants depends on tissue factor and platelets, not FXII or neutrophils. *Blood*. 2019;133(19):2090-9.
33. Cleuren AC, Van der Linden IK, De Visser YP, et al. 17alpha-Ethinylestradiol rapidly alters transcript levels of murine coagulation genes via estrogen receptor alpha. *J Thromb Haemost*. 2010;8(8):1838-46.
34. Schwenk JM, Omenn GS, Sun Z, et al. The Human Plasma Proteome Draft of 2017: Building on the Human Plasma PeptideAtlas from Mass Spectrometry and Complementary Assays. *Journal of proteome research*. 2017;16(12):4299-310.
35. Bhowmick P, Mohammed Y, Borchers CH. MRMAssayDB: an integrated resource for validated targeted proteomics assays. *Bioinformatics*. 2018;34(20):3566-71.

36. Mohammed Y, Bhowmick P, Smith DS, et al. PeptideTracker: A knowledge base for collecting and storing information on protein concentrations in biological tissues. *Proteomics*. 2017;17(7).
37. Mohammed Y, Domanski D, Jackson AM, et al. PeptidePicker: a scientific workflow with web interface for selecting appropriate peptides for targeted proteomics experiments. *J Proteomics*. 2014;106:151-61.
38. Percy AJ, Chambers AG, Yang J, et al. Advances in multiplexed MRM-based protein biomarker quantitation toward clinical utility. *Biochim Biophys Acta*. 2014;1844(5):917-26.
39. MacLean B, Tomazela DM, Shulman N, et al. Skyline: an open source document editor for creating and analyzing targeted proteomics experiments. *Bioinformatics*. 2010;26(7):966-8.
40. Ward JH. Hierarchical Grouping to Optimize an Objective Function. *J Am Stat Assoc*. 1963;58(301):236-&.
41. Murtagh F, Legendre P. Ward's Hierarchical Agglomerative Clustering Method: Which Algorithms Implement Ward's Criterion? *J Classif*. 2014;31(3):274-95.
42. Zhang Q, Menon R, Deutsch EW, et al. A mouse plasma peptide atlas as a resource for disease proteomics. *Genome Biol*. 2008;9(6):R93.
43. Scheurer B, Rittner C, Schneider PM. Expression of the human complement C8 subunits is independently regulated by interleukin 1 beta, interleukin 6, and interferon gamma. *Immunopharmacology*. 1997;38(1-2):167-75.
44. Gruys E, Toussaint MJ, Niewold TA, et al. Acute phase reaction and acute phase proteins. *J Zhejiang Univ Sci B*. 2005;6(11):1045-56.
45. Schreiber G, Tsykin A, Aldred AR, et al. The acute phase response in the rodent. *Ann N Y Acad Sci*. 1989;557:61-85; discussion -6.
46. Ohman-Hanson RA, Cree-Green M, Kelsey MM, et al. Ethnic and Sex Differences in Adiponectin: From Childhood to Adulthood. *J Clin Endocrinol Metab*. 2016;101(12):4808-15.
47. Gaya da Costa M, Poppelaars F, van Kooten C, et al. Age and Sex-Associated Changes of Complement Activity and Complement Levels in a Healthy Caucasian Population. *Front Immunol*. 2018;9:2664.
48. Prakash P, Kulkarni PP, Chauhan AK. Thrombospondin 1 requires von Willebrand factor to modulate arterial thrombosis in mice. *Blood*. 2015;125(2):399-406.
49. Bonnefoy A, Daenens K, Feys HB, et al. Thrombospondin-1 controls vascular platelet recruitment and thrombus adherence in mice by protecting (sub)endothelial VWF from cleavage by ADAMTS13. *Blood*. 2006;107(3):955-64.
50. Lasky LA, Singer MS, Dowbenko D, et al. An endothelial ligand for L-selectin is a novel mucin-like molecule. *Cell*. 1992;69(6):927-38.
51. Dwir O, Shimron F, Chen C, et al. GlyCAM-1 supports leukocyte rolling in flow: evidence for a greater dynamic stability of L-selectin rolling of lymphocytes than of neutrophils. *Cell Adhes Commun*. 1998;6(4):349-70.
52. Wolberg AS. Fibrinogen and factor XIII: newly recognized roles in venous thrombus formation and composition. *Curr Opin Hematol*. 2018;25(5):358-64.
53. Byrnes JR, Duval C, Wang Y, et al. Factor XIIIa-dependent retention of red blood cells in clots is mediated by fibrin alpha-chain crosslinking. *Blood*. 2015;126(16):1940-8.
54. Aleman MM, Byrnes JR, Wang JG, et al. Factor XIII activity mediates red blood cell retention in venous thrombi. *J Clin Invest*. 2014;124(8):3590-600.

55. Conforto TL, Waxman DJ. Sex-specific mouse liver gene expression: genome-wide analysis of developmental changes from pre-pubertal period to young adulthood. *Biol Sex Differ*. 2012;3:9.
56. Jurk K, Clemetson KJ, de Groot PG, et al. Thrombospondin-1 mediates platelet adhesion at high shear via glycoprotein Ib (GPIb): an alternative/backup mechanism to von Willebrand factor. *FASEB J*. 2003;17(11):1490-2.
57. von Bruhl ML, Stark K, Steinhart A, et al. Monocytes, neutrophils, and platelets cooperate to initiate and propagate venous thrombosis in mice in vivo. *J Exp Med*. 2012;209(4):819-35.
58. Maracle CX TJ, Zirka G, Morange PE, van Vlijmen BJM, Thomas GM. Slc44a2 deficient mice exhibit less severity of thrombosis in a stenosis model of DVT. *International Society on Thrombosis & Hemostasis: Research and Practice in Thrombosis and Haemostasis Melboure, Australia, 2019*
59. Maracle CX TJ, Zirka G, van den Heijkant L, Morange PE, van Vlijmen BJM, Thomas GM. Slc44a2 deficient mice exhibit less severity of thrombosis in a stenosis model of DVT. *European Congress on Thrombosis and Haemostasis, Marseille, France, 2018*
60. Constantinescu-Bercu A, Grassi L, Frontini M, et al. Activated αIIbβ3 on platelets mediates flow-dependent NETosis via SLC44A2. *bioRxiv*. 2019:373670.

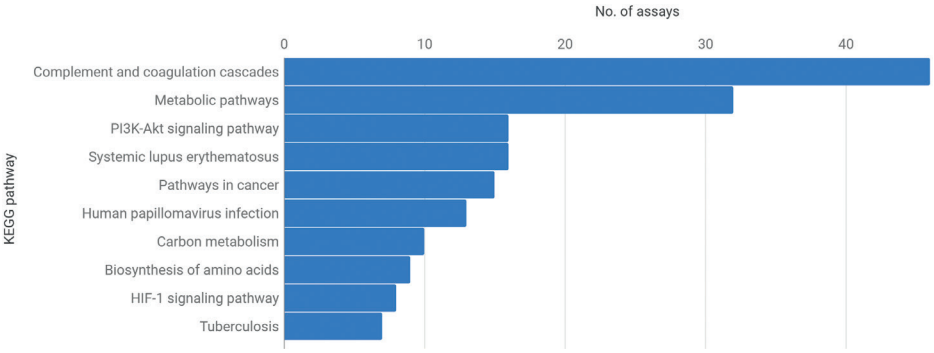

Figure S1. The top 10 biological pathways covered by the used protein assays.

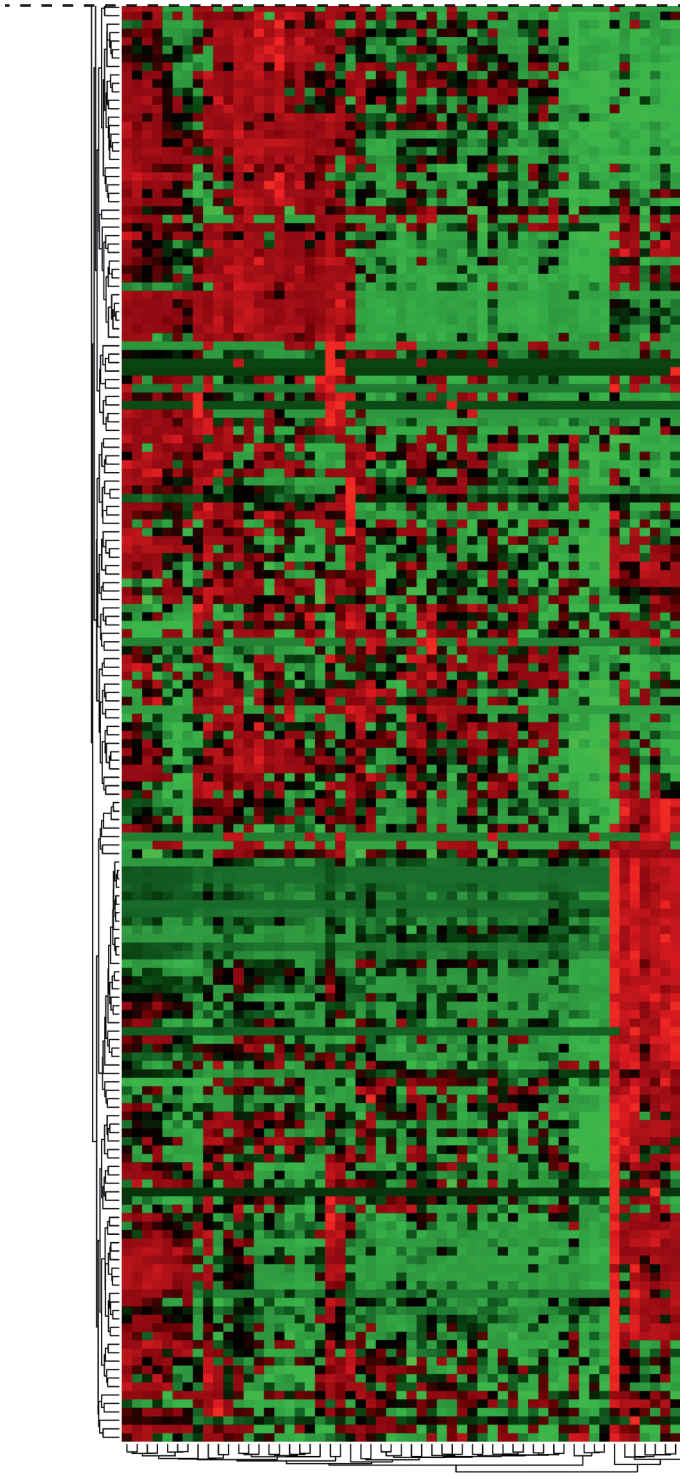

Figure S2. Heatmap showing protein profiles across all included samples annotated with metadata on the experiment, treatment (no treatment, siAT/PC, siControl), sex, and Slc44a2 status (SLC44A2 WT and KO).

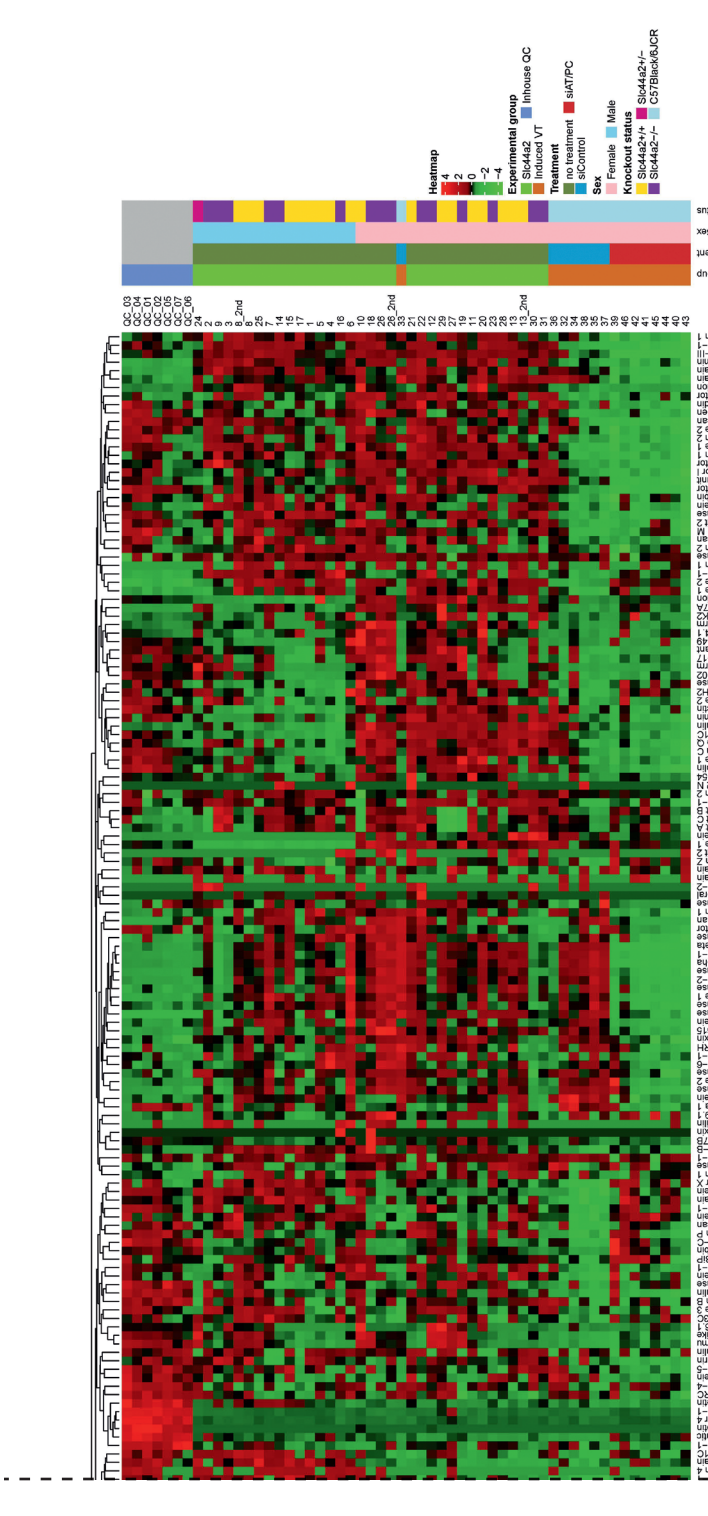

Figure S2 (continued). Heatmap showing protein profiles across all included samples annotated with metadata on the experiment, treatment (no treatment, siAT/PC, siControl), sex, and Slc44a2 status (SLC44A2 WT and KO).

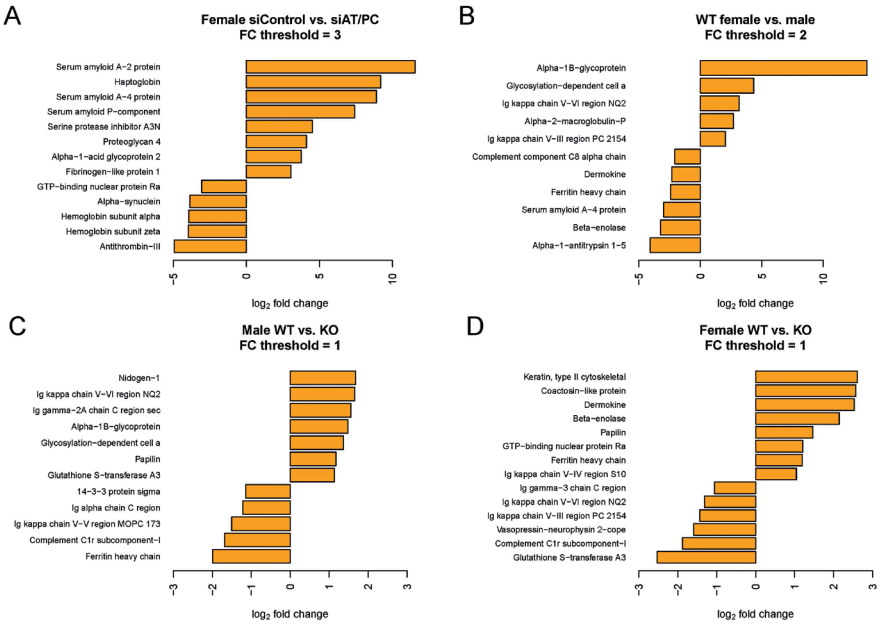

Figure S3. Fold changes in protein abundancy of (A) siAT/PC vs. siControl proteins with higher fold changes than log2 3 are displayed. (B) male vs. female proteins with higher fold changes than log2 2 are displayed. (C) male Slc44a2-/- (KO) vs. male Slc44a12+/+ (WT) proteins with higher fold changes than log2 1 are displayed. (D) female Slc44a2-/- (KO) vs. female Slc44a2+/+ (WT) proteins with higher fold changes than log2 1 are displayed.

Table S1 Proteins and surrogate peptides used in our quantitative targeted proteomics method

Table is available in online supplement.

Table S2. Weight change of mice treated with siAT/PC and siControl.

					Weigth (gram)					
Mouse #	Strain	Sex	Age (weeks)	Treatment	at siRNA injection	24 hrs post injection	32 hrs post injection	At sacrifice	Delta (injection to sacrifice)	Clinical signs (hr. post injection)
32	C57BLACK/6J	Female	6	siControl	21,4	21,3	21,7	21,1	-0,3	N/A
33	C57BLACK/6J	Female	6	siControl	18,7	19,2	19,7	19,8	1,1	N/A
34	C57BLACK/6J	Female	6	siControl	20,7	21,1	21,4	21,9	1,2	N/A
35	C57BLACK/6J	Female	6	siControl	21,9	22,0	22,0	22,3	0,4	N/A
36	C57BLACK/6J	Female	6	siControl	21,1	20,9	21,3	20,7	-0,4	N/A
37	C57BLACK/6J	Female	6	siControl	21,6	20,5	20,8	21,3	-0,3	N/A
38	C57BLACK/6J	Female	6	siControl	20,0	20,0	20,7	20,6	0,6	N/A
39	C57BLACK/6J	Female	6	siAT/PC	18,7	17,9	17,4	16,1	-2,6	65
40	C57BLACK/6J	Female	6	siAT/PC	20,7	20,4	20,8	18,4	-2,3	65
41	C57BLACK/6J	Female	6	siAT/PC	19,9	19,9	18,9	18,2	-1,7	44
42	C57BLACK/6J	Female	6	siAT/PC	20,9	20,6	20,1	17,5	-3,4	65
43	C57BLACK/6J	Female	6	siAT/PC	19,5	19,5	19,3	17,2	-2,3	65
44	C57BLACK/6J	Female	6	siAT/PC	21,1	20,6	19,3	18,7	-2,4	44
45	C57BLACK/6J	Female	6	siAT/PC	20,7	21,1	21,6	19,3	-1,4	65
46	C57BLACK/6J	Female	6	siAT/PC	20,0	20,0	20,4	18,3	-1,7	66

Table S3. Weight of the *Slc44a2* KO mice as well as wild type littermates at sacrifice.

Mouse #	Age (weeks)	Sex	Genotype	Body weigth at sacrifice (gram)
11	15	Female	WT	24,8
21	15	Female	WT	22,5
10	15	Female	WT	21,2
27	15	Female	WT	18,3
20	15	Female	WT	23,3
13	15	Female	WT	23,5
28	15	Female	WT	20,1
29	15	Female	WT	20,4
22	15	Female	KO	21,3
31	15	Female	KO	22,7
12	15	Female	KO	21,9
18	15	Female	KO	22,5
23	15	Female	KO	22,2
26	15	Female	KO	21,4
19	15	Female	KO	21,9
30	15	Female	KO	24,9
6	15	Male	WT	28,3
17	15	Male	WT	28,9
1	15	Male	WT	27,2
15	15	Male	WT	30,7
25	15	Male	WT	28,4
4	15	Male	WT	29,7
8	15	Male	WT	31,7
5	15	Male	WT	31,1
24	15	Male	HET	27,0
14	15	Male	KO	35,2
16	15	Male	KO	31,2
3	15	Male	KO	30,5
9	15	Male	KO	24,7
2	15	Male	KO	29,6
7	15	Male	KO	27,7